Soil Dynamics and Earthquake Engineering 79 (2015) 280–295

Contents lists available at ScienceDirect

Soil Dynamics and Earthquake Engineering

journal homepage: www.elsevier.com/locate/soildyn

Liquefaction-induced ground damages during the 2010 Chile earthquake

Ramón Verdugo*, Javiera González

[a] Principal of CMGI – Chile, Alameda 2356, Santiago, Chile
[b] University of Chile, Beaucheff 850, Santiago, Chile

ARTICLE INFO

Article history:
Received 30 July 2014
Received in revised form
10 April 2015
Accepted 21 April 2015
Available online 19 May 2015

Keywords:
Earthquake geotechnical engineering
Liquefaction
2010 Chile earthquake

ABSTRACT

The second-strongest earthquake recorded in Chile's history, only exceeded by the 1960 Valdivia earthquake of Magnitude 9.5, occurred on February 27, 2010. This mega thrust-faulting type earthquake of Magnitude 8.8 struck the Central-South region. The shaking duration of each acceleration record was computed, and the longest records were coincident with the area of maximum crustal co-seismic deformations. Liquefaction sites covered an extension close to 1000 km, which approximately represents twice the length of the rupture zone. It was confirmed that tailings dams built using the upstream construction method are seismically unsafe, thus efforts must be done by governments in order to identify and prevent failures of existing old tailings dams. On the other hand, it is shown that in high seismic regions a stratified structure consisting of a sequence of loose (liquefiable) and dense (non-liquefiable) sandy layers should be expected, making the analysis more complex.

1. Introduction

The 2010 decade has been particularly active in terms of destructive earthquakes, i.e. Haiti 2010 (Mw=7.0); Chile 2010 (Mw=8.8), New Zealand 2011 (Mw=6.3) and Japan 2011 (Mw=9.0). All of these earthquakes have left significant damages to properties and loss of human lives. Although important technical achievements have been accomplished in the last decades in the field of earthquake geotechnical engineering, significant seismic damages still occur in seismic areas around the world. In economic terms, the 2010 Chile Earthquake has been the worst natural disaster in Chile's history, with a total cost of about 30 billion US dollars. This economic damage is equivalent to near 18% of the Chilean gross domestic product (GDP). Both the earthquake and the tsunami caused near 600 casualties.

One of the causes of the resulting damages is associated with soil liquefaction, and the significant soil displacements that are characteristic of this phenomenon. The 2010 Chile Earthquake has repeated the catastrophic experience left by large earthquakes in other highly seismic areas, including the occurrence of soil liquefaction at several sites. Significant damages were reported in road infrastructure, railroads system, ports, buildings and houses, agriculture terrains, irrigation channels, tailings dams, among others. The failures of pile foundations induced by lateral spreading produced a serious impact on the operation of ports and industrial buildings. The operation disruption of these facilities produced a much higher cost than the rehabilitation of the substructures.

The 2010 Chile earthquake is among the six largest seismic events that have been instrumentally recorded in the world. Accordingly, the learnings from this earthquake are of great value for geotechnical engineering as well as other disciplines. The field observations and the analysis of the available data provide a unique set of information and new insights concerning the actual seismic behavior of soil deposits.

This article presents the results of a comprehensive investigation that allowed the identification of over 170 sites, where evidence of liquefaction was observed, covering an extension of nearly 1000 km. Reconnaissance of the affected area, interviews with local witnesses, reports from city halls, and newspapers, permitted to appreciate how vast the extension of the liquefaction phenomena really was.

The available acceleration records of the 2010 Chilean Earthquake were analyzed and their durations computed. It is shown in the paper that the durations vary significantly, being larger around the area where important co-seismic crustal deformations were measured.

Additionally, empirical evidences show that in highly seismic environments, any sandy soil deposit, initially loose and saturated, should undergo liquefaction during its geological time. The repetitive liquefaction episodes create highly heterogeneous soil deposits, at least in terms of density profile. Therefore, in regions of high seismicity,

* Corresponding author. Tel.: +56 2 25690755.
E-mail addresses: rverdugo@cmgi.cl (R. Verdugo), javigonz@ing.uchile.cl (J. González).

http://dx.doi.org/10.1016/j.soildyn.2015.04.016
0267-7261/

liquefiable soil deposits are always strongly stratified, making its analysis more complex.

2. The 2010 Chile earthquake

On February 27, 2010, at 3:34 am, local time, a mega earthquake of Magnitude Mw=8.8 struck off the south central part of Chile. The earthquake was followed by a tsunami that severely affected several cities and towns along the coast. After the main shock a long series of aftershocks continued striking the region, being the most important one of Magnitude 6.2 which occurred 20 min after the main shaking.

The 2010 Chile earthquake is the second-strongest recorded in the nation's history, only exceeded by the 1960 Valdivia earthquake of Magnitude 9.5, which so far is the largest earthquake ever recorded. These two mega thrust-faulting type earthquakes originated in the boundary between the subducting Nazca Plate and the overriding South American Plate.

According to USGS (United States Geological Survey), the hypocenter corresponding to the initiation of the process of rupture was located at 35.909 °S and 72.733 °W at a depth of 35 km. The rupture zone responsible for this earthquake compromised a rectangular area of approximately 550 km by 170 km (Fig. 1) on the interface between the two plates, at an average depth of 35 km. The southern end of the rupture zone overlapped the rupture zone of the 1960 Valdivia earthquake and stopped near the southern end of the 1985 Valparaíso earthquakes of Mw 8.0 [1].

Using data generated by a Global Positioning System (GPS) networks installed in the epicentral area, Vigny et al. [2] determined that the rupture propagated bilaterally from the hypocenter at about 3.1 km/s, with a slip up to 15 m in the north area of the rupture. Additionally, they reported the co-seismic crustal deformations showed in Fig. 2, where the arrows and numbers indicate the direction and magnitude of the displacements in centimeters, respectively. A cross section displaying the distribution of the vertical displacements from the trench toward the continent is presented in Fig. 3. The red circles are associated with deformations near Constitución latitude (35.5 °S to 36 °S), while green circles represent values obtained near Arauco-Concepción latitude (37 °S to 37.5 °S); intermediate latitudes are represented by white circles. The solid line attempts to give an idea of the overall trend [2].

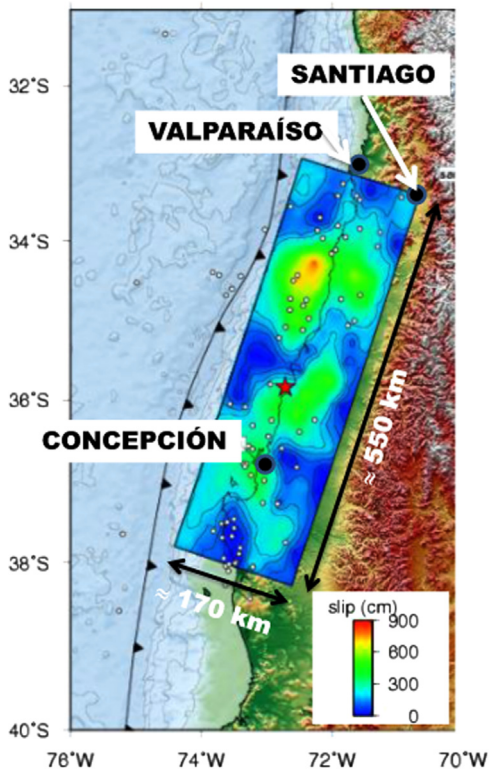

Fig. 1. Rupture zone of 2010 Chile Earthquake (modified from www.tectonics.caltech.edu/slip_history).

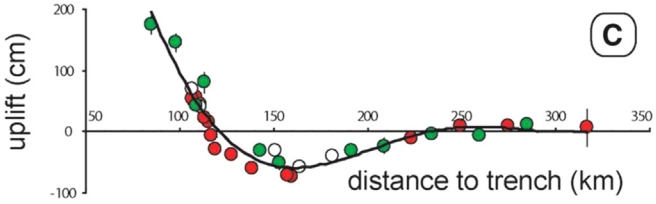

Fig. 3. Land-level changes as a function of distance to the trench. Ref. [2].

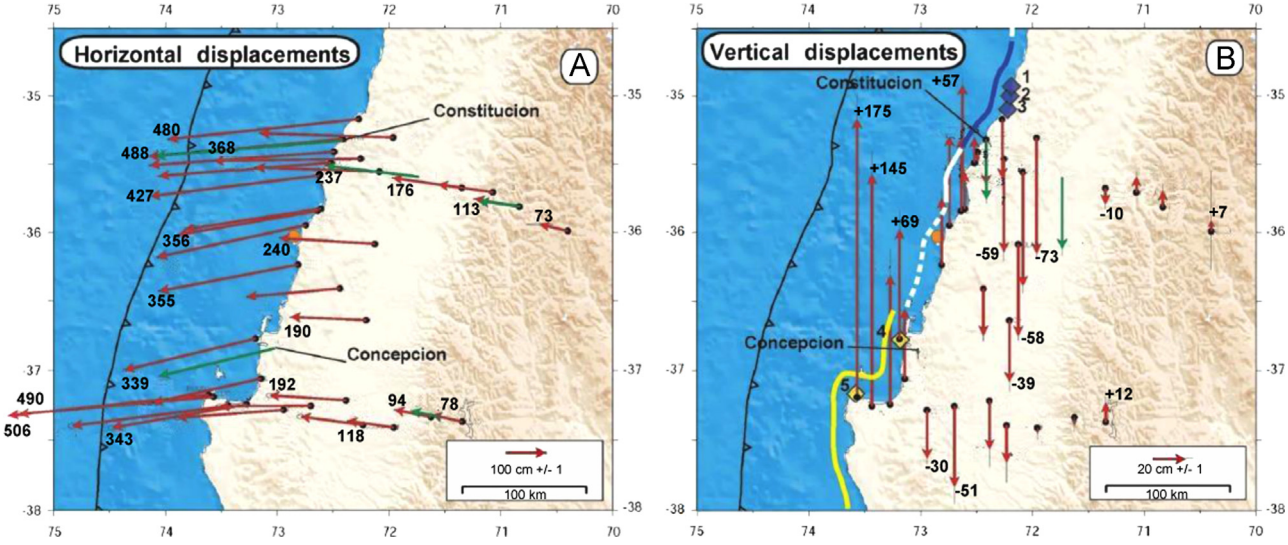

Fig. 2. Co-seismic static displacement field. Survey sites (red arrows) and continuous Global Positioning System stations (green arrows) (modified from [2]).

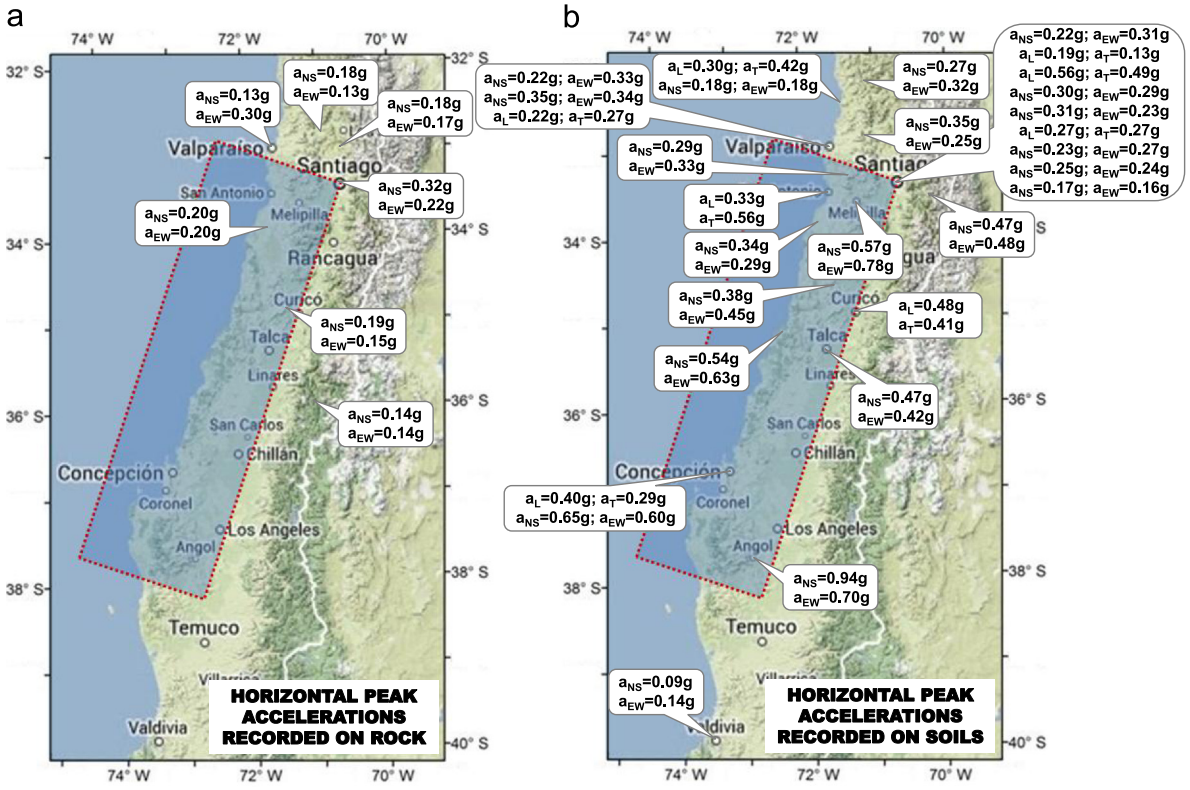

Fig. 4. Horizontal PGAs recorded on (a) rock outcrops and (b) soil deposits. Data from [3] and [4].

It is of a great interest to observe that at the tip of Arauco Peninsula, the permanent deformations measured after the earthquake reached an uplift of 1.8 m and a horizontal displacement of 5.1 m towards the trench. These significant deformations, currently observed after major earthquakes, could be responsible of the longer durations observed in the acceleration records, as discussed next.

3. Characteristic of acceleration records

The 2010 Chile earthquake is among the few large events ever recorded with modern instruments. Close to 40 seismic stations located in the most affected area recorded the acceleration time histories on both rock outcrops (sites where the rock mass can be clearly observed on the surface) and soil deposits (sites where the bedrock is deeper than 20 m) of different geotechnical characteristics. The horizontal maximum accelerations recorded on rock outcrops and soil deposits are presented in Fig. 4.

The horizontal peak ground accelerations (PGA) obtained on rock outcrops are unexpectedly moderate, with a maximum value of 0.32 g recorded in Santa Lucía Hill site located in the center of Santiago. Unfortunately, no instruments placed on rock outcrops were available toward the south, where higher values of PGA could be expected.

On the other hand, the horizontal PGA's recorded on soil deposits were significantly higher, reaching a maximum value of 0.94 g in Angol, corresponding to a site that is located close to the south end of the rupture zone. Interestingly, the second highest value of PGA was 0.78 g, recorded in the city of Melipilla, which is located close to the north end of the rupture zone.

Regarding the duration of shaking on soil deposits, the available records clearly show a significant variation depending on their location (Fig. 5). These data do not support the well accepted concept that the duration of a strong motion is mainly a function of the earthquake magnitude. It is important to mention that in the area affected by the 2010 Chile Earthquake, the basins and valleys are rather shallow, with less than 0.4 km in depth, and several kilometers in any horizontal direction. Therefore, the geometry of these basins and valleys is similar to a thin plate, where reverberation of seismic waves trapped in the soil deposit should not be significant enough to increase the duration of shaking.

Different approaches to estimate the portion of the accelerograms that represents its duration for engineering purposes have been proposed ([5–8] among others). In this study the Arias Intensity [9] has been adopted to establish the duration of each acceleration time history record. The Arias Intensity function, $I_a(t)$, is defined as:

$$I_a(t) = \frac{\pi}{2g}\int_0^t [a(t)]^2\ dt \tag{1}$$

where g is the acceleration of gravity and $a(t)$ is the acceleration-time history in units of g.

Trifunac and Brady [6] suggested that the interval between 5% and 95% of the Arias intensity provides an appropriate indicator for the significant duration of an accelerogram. Therefore, the duration of a shaking is evaluated by computing the time interval $\Delta t = t_2 - t_1$, where:

$$I_{a-5\%} = I_a(t_1) = 0.05 \cdot I_a^{\max} \tag{2}$$

$$I_{a-95\%} = I_a(t_2) = 0.95 \cdot I_a^{\max} \tag{3}$$

$$I_a^{\max} = \frac{\pi}{2g}\int_0^{\infty} [a(t)]^2\ dt (\text{Arias Intensity}) \tag{4}$$

The obtained durations, Δt_a, for the available records are presented in Table 1. Alternatively, it was considered that the initiation time in each acceleration record should be associated with the same level of seismic energy, a kind of triggering to all the records, which permits to standardize the analysis for the same seismic event. Considering that the Arias Intensity is associated with the seismic energy [9] a unique value of $I_{a\text{-}5\%}$ was

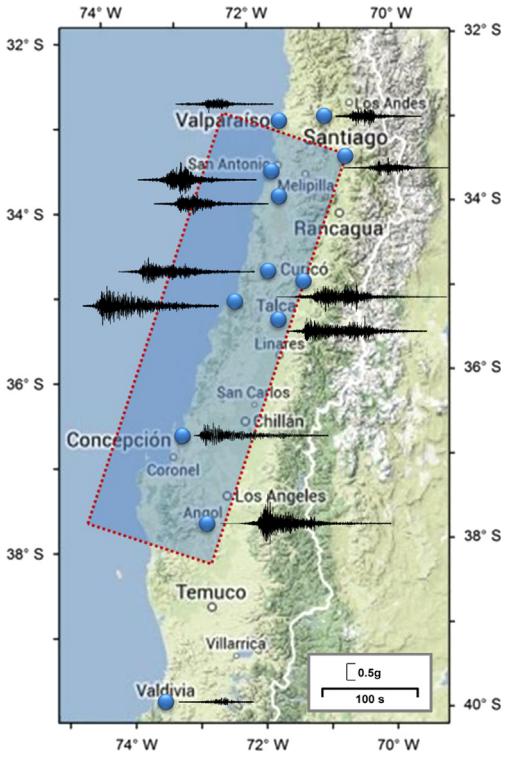

Fig. 5. Recorded acceleration time histories at different location. Data from [3] and [4].

established as reference for all the accelerograms. For each acceleration record, the value corresponding to 5% of the Arias intensity was computed, then, the lowest value was selected to be used as reference (Valdivia).

The duration for engineering purposes was considered such that the two horizontal components can be separately treated and assumed to be independent of each other. Accordingly, the Arias intensity was calculated for each component and the corresponding durations computed. The shaking durations obtained with this procedure; Δt_b, are presented in Table 1. It can be observed that the general trend is similar for both procedures, with longer durations associated with an initial common level of seismic energy.

The resulting durations of the available accelerograms, Δt_b, are presented in Fig. 6. It can be observed that the longer records took place in the vicinity of Concepción, coinciding with the region where the greatest co-seismic deformations were detected (Fig. 6). According to these results, the accelerogram of Concepción has the longest duration with 91 s, while Valdivia has the shortest duration with 30 s. These two acceleration histories and the corresponding Arias Intensity functions are presented in Fig. 7. Additionally, in Fig. 8 are shown the data from other earthquakes that also confirm the variation of shaking duration for a given magnitude.

There are studies indicating that, in addition to the magnitude of the earthquake, factors such as site-source distance and site parameters affect the earthquake duration that is of engineering interest. However, the obtained data suggest that for large earthquakes, that duration would also be controlled by the extension of the zone where the greatest co-seismic crustal deformations take place.

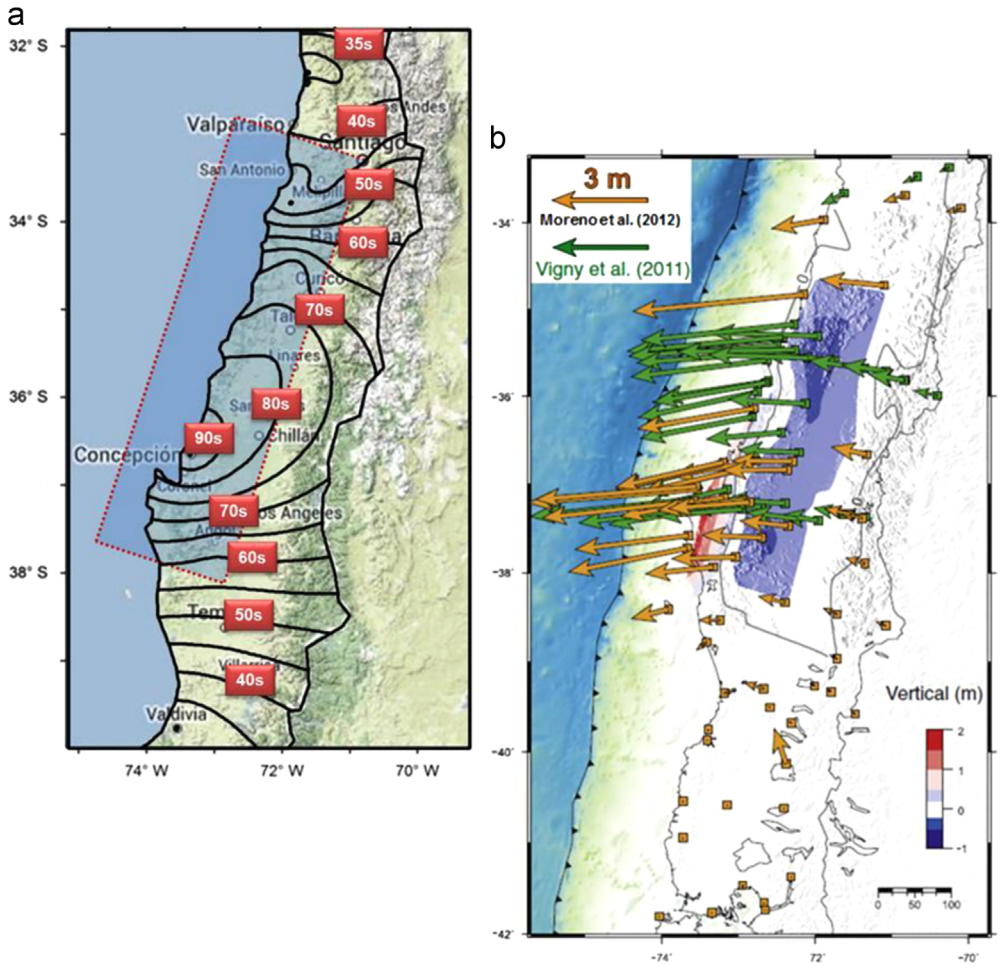

Fig. 6. (a) Contours of duration Δt_b and (b) co-seismic deformations [10].

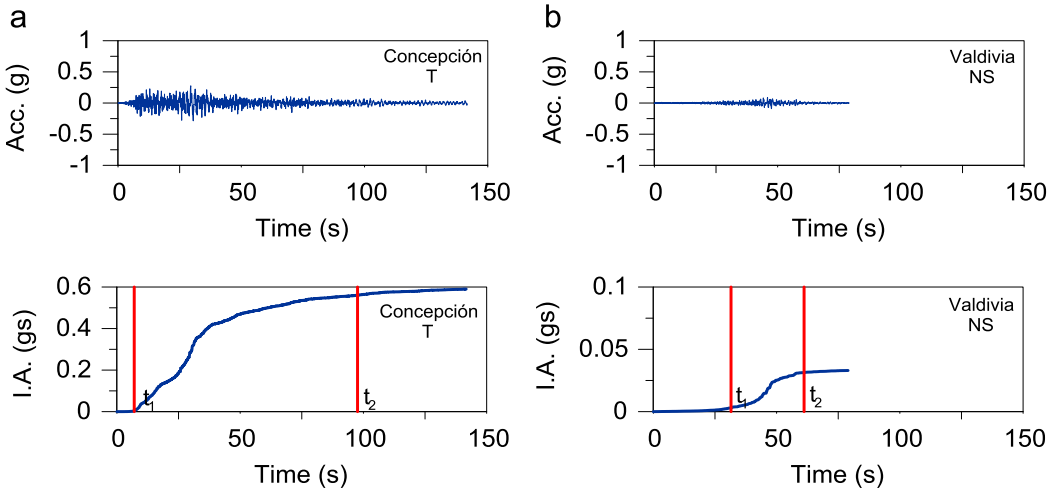

Fig. 7. Accelerograms and Arias Intensity of (a) Concepción and (b) Valdivia. Data from [3] and [4].

Table 1
PGA, Arias Intensity and durations of recorded accelerations.

CITY	LOCATION (°)		PGA	I_a	Δt_a	Δt_b
	LATITUDE	LONGITUDE	(g)	(g s)	(s)	(s)
Cabildo	32.43	71.07	0.27 0.32 0.13	0.27 0.27	30.85 31.37	41.82 41.85
Papudo (Azimuth: 60°)	32.51	71.45	0.30 0.42 0.16	0.29 0.40	29.07 28.28	44.48 48.38
Zapallar	32.55	71.46	0.18 0.18 0.11	0.06 0.06	31.08 30.31	31.20 30.13
Olmué	33.00	71.19	0.35 0.25 0.15	0.41 0.20	27.61 32.11	35.11 37.84
Viña Centro	33.03	71.55	0.22 0.33 0.18	0.21 0.39	29.31 24.58	38.63 35.91
Viña El Salto	33.05	71.51	0.35 0.34 0.26	0.45 0.48	30.45 33.55	45.96 48.17
Valpo. Almendral (Azimuth: 310°)	33.05	71.62	0.22 0.27 0.14	0.23 0.21	31.00 26.97	41.23 41.77
Casablanca	33.32	71.41	0.29 0.33 0.23	0.38 0.39	32.19 30.08	39.90 35.01
Stgo - Las Américas	33.45	70.53	0.31 0.23 0.16	0.39 0.31	37.44 39.31	50.14 51.78
Stgo – FCFM	33.46	70.66	0.17 0.16 0.14	0.12 0.13	39.10 38.70	41.14 40.09
Stgo Centro	33.47	70.65	0.22 0.31 0.18	0.22 0.27	35.22 34.11	43.75 39.46
Stgo - FSR	33.48	70.53	0.25 0.24 0.18	0.35 0.30	42.44 43.50	55.12 52.04
Stgo – Maipú (Azimuth: 340°)	33.51	70.77	0.56 0.49 0.24	0.59 0.50	32.10 33.78	43.63 45.42
Stgo – Peñalolén	33.50	70.58	0.30 0.29	0.33 0.34	33.69 34.19	40.01 47.13

Table 1 (*continued*)

CITY	LOCATION (°)		PGA	I_a	Δt_a	Δt_b
	LATITUDE	LONGITUDE	(g)	(g s)	(s)	(s)
			0.28			
Stgo – La Florida (Azimuth: 321°)	33.51	70.61	0.19	0.10	39.91	43.19
			0.13	0.10	41.56	44.57
			0.10			
Stgo – Antumapu	33.57	70.63	0.23	0.19	38.56	43.38
			0.27	0.21	38.46	43.18
			0.16			
Stgo – Puente Alto (Azimuth: 22°)	33.58	70.58	0.27	0.26	36.23	41.46
			0.27	0.17	37.95	41.79
			0.13			
San José	33.64	70.35	0.47	0.67	38.39	57.47
			0.48	0.77	39.00	56.33
			0.25			
Llolleo (Azimuth: 340°)	33.62	71.60	0.33	0.50	36.33	48.64
			0.56	1.03	32.00	47.62
			0.68			
Melipilla	33.69	71.21	0.57	0.92	31.97	41.11
			0.78	1.29	31.80	38.44
			0.39			
Matanzas	33.96	71.87	0.34	0.72	34.02	42.09
			0.29	0.46	34.96	44.22
			0.24			
Hualañe	34.98	71.87	0.38	0.79	61.67	74.43
			0.45	0.87	56.03	63.89
			0.38			
Curicó (Azimuth: 150°)	34.98	71.24	0.48	1.09	50.19	66.32
			0.41	1.12	51.57	66.65
			0.20			
Constitución	35.34	72.41	0.54	2.01	59.79	67.50
			0.63	2.65	65.23	73.90
			0.35			
Talca	35.43	71.66	0.47	1.16	69.86	77.24
			0.42	1.10	71.94	79.63
			0.22			
Concepción (Azimuth: 60°)	36.83	73.05	0.40	0.89	80.69	84.18
			0.29	0.58	88.21	90.59
			0.37			
San Pedro	36.84	73.11	0.65	1.77	69.91	73.20
			0.60	1.46	74.62	78.79
			0.58			
Angol	37.79	72.71	0.94	2.03	50.82	61.90
			0.70	1.78	49.76	58.91
			0.29			
Valdivia	39.83	73.24	0.09	0.03	33.87	29.64
			0.14	0.06	29.03	29.03
			0.05			

Δt_a:Significant Duration.
Δt_b:Significant Duration using the same minimum $I_{a-5\%}$.
PGA N-S or L.
E-W or T.
Vertical.
The orientations of the horizontal axis of some instruments were close, but not exactly, in the N-S and E-W directions. In these cases, the components L (longitudinal) and T (transversal) represent the closest direction to N-S and E-W components, respectively. The azimuth is indicated for these instruments.

4. Geology of the central-south region of Chile

As shown in Fig. 9, to the south of 33 °S latitude approximately, the geology of Chile is characterized by the existence of three clear morphostructural units running parallel to each other with a north–south orientation. From east to west, these units are Andes Mountain Range, Central Valley (or Intermediate Depression) and Coastal Mountain Range.

The Andes Mountain Range is located at the east of the country, and it can be seen as a natural barrier that exists along virtually all

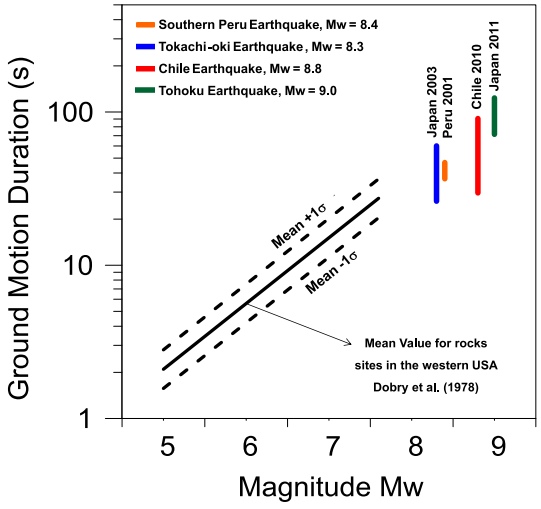

Fig. 8. Relationship between ground motion duration and earthquake magnitude (modified from [11] and [12]).

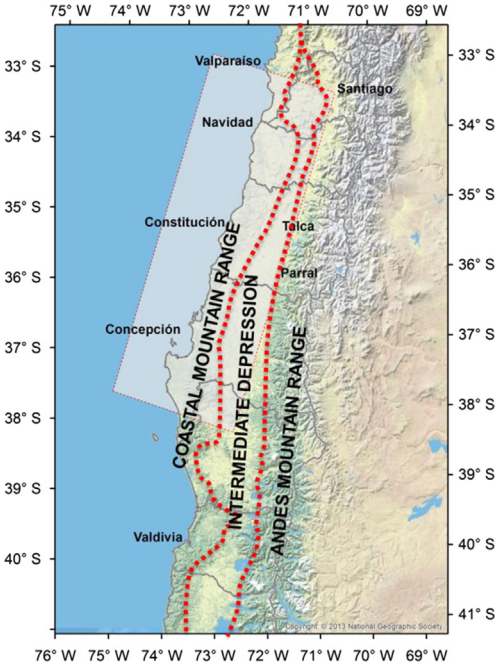

Fig. 9. Main morphostructural units in Central-South Chile.

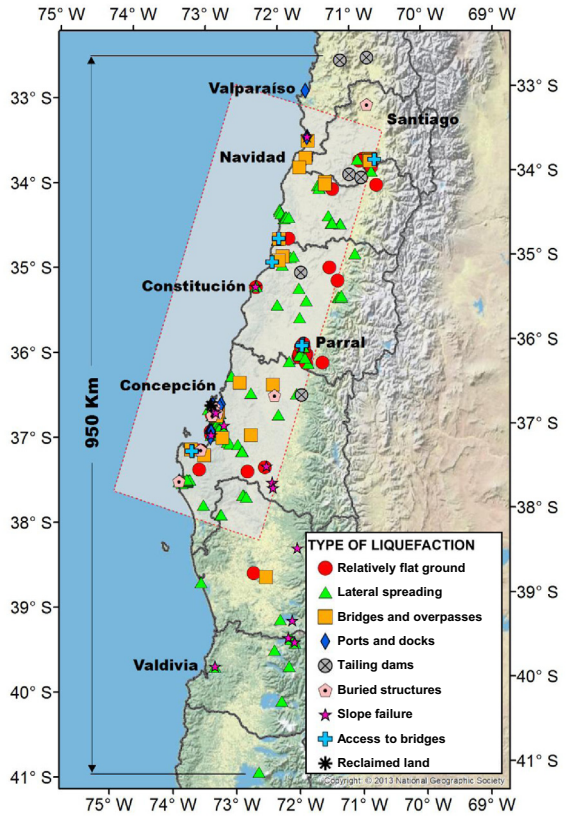

Fig. 10. Sites with evidence of liquefaction.

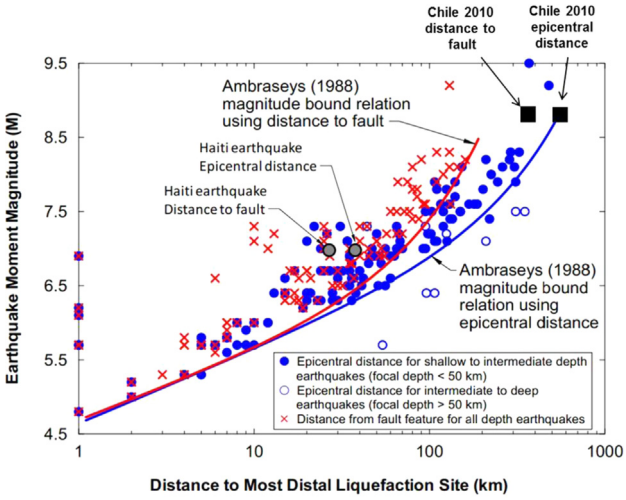

Fig. 11. Earthquake Magnitude and distances to most distal liquefaction sites (modified from [14] and [15]).

Fig. 12. Liquefaction in Muelle Schuster at Valdivia City: (a) 1960 Valdivia Earthquake (El Mercurio) and (b) 2010 Chile Earthquake (Sernageomin).

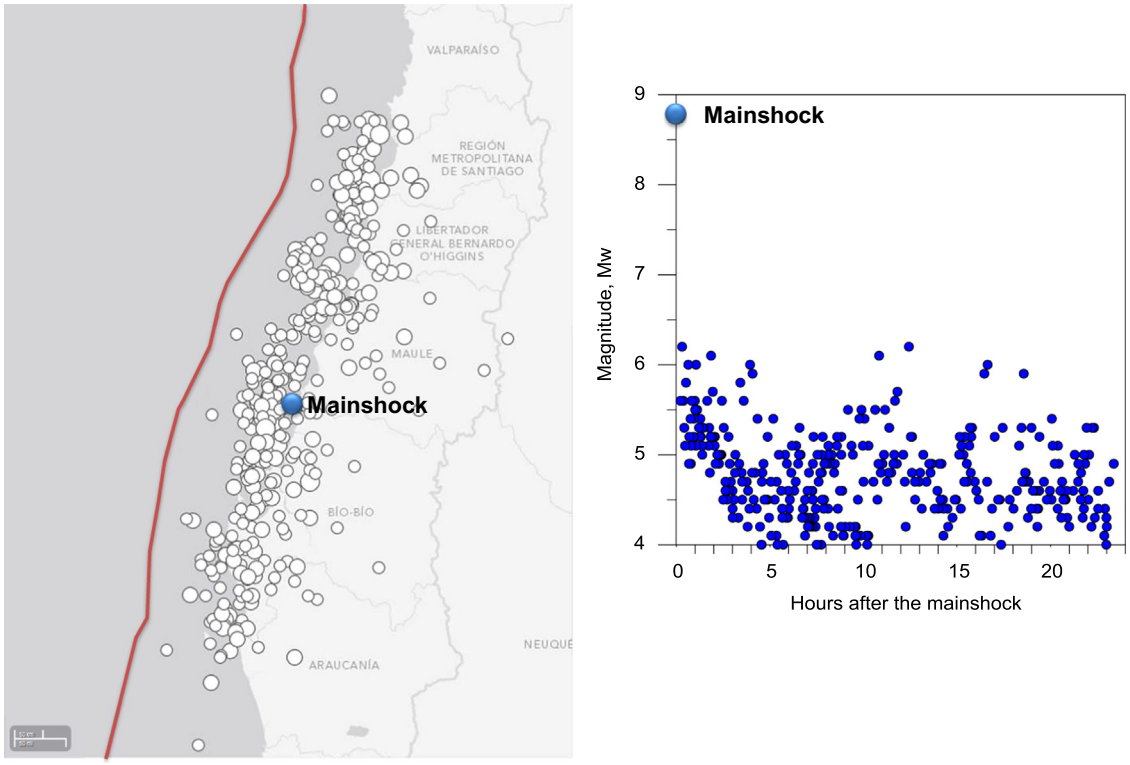

Fig. 13. Aftershocks during the first 24 h. Data from USGS.

Fig. 14. Post-liquefaction settlements. (a) Costanera route in Concepción and (b) near Concepción City (EFE).

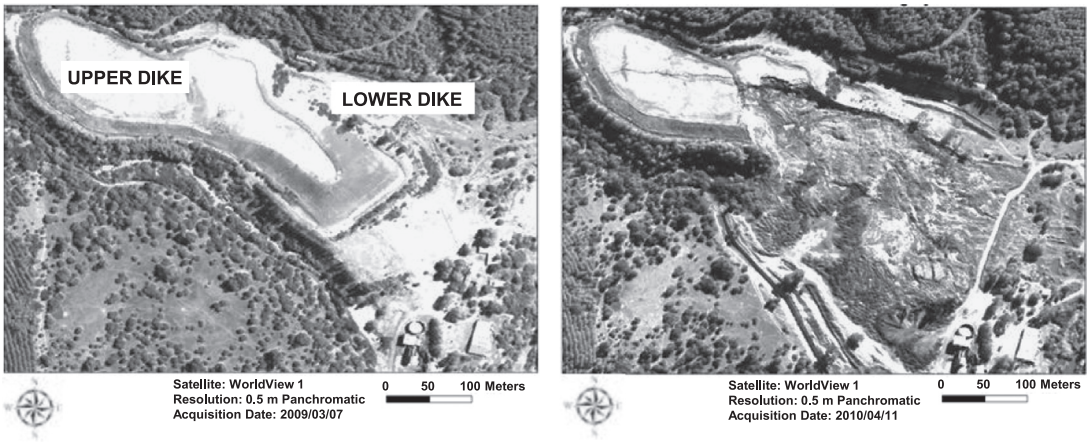

Fig. 15. Before and after failure of Las Palmas tailings dam (modified from [19]).

Chilean territory, disappearing under the sea far south at Cape Horn (it emerges again in the Antarctic). The two tallest mountains are Aconcagua (6959 m.a.s.l.) and Nevado Ojos del Salado (6880 m.a.s.l.). From Santiago to the south, the altitude of the Andes progressively loses height, from 6000 m.a.s.l., in the vicinity of Santiago, to 3000 m.a.s.l. around 37 °S latitude. Along the Andes

Range, there is a major volcanic activity which is remarkable towards south. The existence in Chile of more than 40 active volcanic groups is indicative of this singular condition. Eruptions are frequent and usually violent amongst the 25 active volcanoes located in the Southern Andes [13].

The Coastal Mountain Range extends from Camaraca Mountain, located 20 km south of Arica (close to 19°S latitude), to the Taitao Peninsula (47°S latitude). In the central area, it presents heights that rise above 2000 m.a.s.l. and progressively decreasing southward. There are a significant number of narrow valleys across the Costal Range created by the flow of rivers, along which sandy soil deposits are quite recurrent. These types of soil deposits are also found along the coast line, where an important number of cities and towns are located.

The Central Valley is a depression existing between both the Coastal Mountain Range and the Andes Mountains Range, which is shortly interrupted by the transverse valleys and sunk beneath sea level approximately at 42 °S. It reappears at north of Santiago, from where the valley widens, although it undergoes several reductions at different locations. In the area affected by the 2010 Chile earthquake, the Intermediate Depression is partially covered with glacio-fluvial sediments from the Andes and soils derived from volcanic ashes. Along the banks of rivers that run from Andes Mountain to the sea, the existence of sandy soil deposits is frequent. Also, in surroundings lakes, sandy soil deposits with a shallow water table are commonly found.

Therefore, sites composed of saturated sandy liquefiable soil deposits are mainly located in the Intermediate Depression, as well as along the valleys that pass throughout the Coastal Range, and along the coast line.

5. Overview of the observed liquefaction

After an extensive fieldwork reconnaissance and a comprehensive review of local newspapers, several sites affected by liquefaction were identified and incorporated to the data base. As a result, more than 170 sites with clear evidence of liquefaction have been recognized, which are identified in Fig. 10. It can be observed that the region affected by liquefaction covers an area with a length close to 1000 km in the North–South direction, which represents approximately twice the length of the rupture zone. This is considered an exceptionally vast region subjected to the phenomenon of liquefaction, involving numerous sites.

It is interesting to observe that the sites that experienced liquefaction did not extend symmetrically from the rupture zone. Liquefied soil deposits were observed well to the south of the rupture zone, while to the north of the rupture zone only few cases were found, which cover a reduced area. it is important to mention that to the south of the rupture zone, lateral spreading corresponds to most of the cases reported, which were typically observed in the borders of lakes.

The farthest site that experienced liquefaction is located to the south-east of Valdivia city, in a border of Llanquihue Lake, approximately at 550 km from the epicenter and 350 km from the fault. The distances to the most distal liquefaction site has been reported as a function of the earthquake magnitude [14,15]. This empirical relationship is shown in Fig. 11, where the farthest liquefaction site observed during the 2010 Chile Earthquake is included. As it can be observed, there is a good agreement with the epicentral distance, while the prediction for the distance to fault is underestimated.

The more frequent occurrence of liquefaction in the southern zone can partially be explained by the existence of numerous saturated sandy soil deposits in this area, especially bordering lakes. On the contrary, toward the north the climate is arid with phreatic surfaces usually quite deep and soil deposits mostly constituted by coarse materials in a fine matrix.

Nonetheless, considering the fairly moderate level of accelerations recorded in Valdivia (PGA=0.14 g), the liquefaction observed in this city and surroundings is rather difficult to explain. A singular condition of this area is associated with the fact that it has been previously subjected to a mega earthquake of magnitude 9.5 (1960 Valdivia Earthquake), which also induced liquefaction in several sites. It is possible to venture that previously-liquefied soil deposits may remain in a susceptible condition to liquefy again. One example is presented in Fig. 12. The same site (Muelle Schuster) located in Valdivia City was affected by important

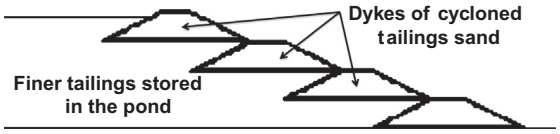

Fig. 16. Upstream tailings dam construction method.

Fig. 17. Lateral spreading observed in (a) Apalta route (http://sites.google.com/site/valledeapalta), (b) Lo Custodio Lagoon, near Concepción (http://losandes-concepcion.blogspot.com) and (c) Itata river.

Fig. 18. Lateral spreading, (a) Coronel Port, (b) Bocamina Port and (c) Fishermen's Port.

liquefaction-induced damages during the 1960 Valdivia Earthquake, and also during the 2010 Chile Earthquake.

On the other hand, the almost 1000 km zone along the country with sites that experienced liquefaction might raise the valid question of whether the aftershocks could also be responsible for some of these events. The series of aftershocks of Magnitude greater than 4.0 that occurred during the first 24 h are presented in Fig. 13. The most important recorded aftershock had a Magnitude 6.2, and occurred 20 min after the main shock. The others aftershocks were mostly of Magnitudes lower than 6.0.

The normal seismicity in Chile is such that all the area affected by liquefaction is repeatedly subjected to earthquakes of similar magnitudes, and even higher, to those reported in the series of aftershocks. Furthermore, liquefaction phenomena have never been reported after these earthquakes, therefore, the aftershocks should not be responsible of additional liquefied sites. Additionally, as far as the authors are aware, all witnesses have indicated that the onset of liquefaction was associated with the mainshock. Therefore, it is possible to conclude that the vast extension of liquefied sites was primarily related to the main seismic event of Magnitude 8.8.

It is interesting to mention that the liquefaction sites observed during the 2010 Chile Earthquake were mainly associated with natural ground. This fact is different from what happened during the 2011 Great East Japan Earthquake, where liquefaction was concentrated in man-made fill associated with reclaimed land ([16]).

6. Cases of severe liquefaction

6.1. Post-liquefaction settlements

The post-liquefaction scenario on rather flat terrains was characterized by important settlements that developed on the ground surfaces. For the particular geological and geotechnical characteristics of the affected area, the field observation suggests that maximum settlements of natural ground are limited to 1.5 m. The photos presented in Fig. 14 show typical cases of post-liquefaction settlements developed on horizontal grounds.

6.2. Collapse of las Palmas tailings dam

In the area affected by the 2010 Chile Earthquake there were seven major tailings deposits and more than 50 small to medium tailings dams, some of which had limited engineering design. The major dams presented no seismic damages, except for some longitudinal cracks along the crest.

On the other hand, only four of the existing medium tailings dams developed limited damages, and Las Palmas tailings dams experienced a liquefaction-induced flow failure [17,18]. The liquefied tailings flowed downstream about 400 m, contaminating the area and causing four fatalities. The victims were buried inside their home under 4 m of tailings (Fig. 15). In situ measurements on the remaining tailings indicated shear wave velocities in the order of 250 m/s, and dynamic cone penetrometer soundings yielded blow counts of about 10 [20].

Las Palmas tailings deposit consisted of two dams (lower and upper) that were constructed in stages using the upstream construction method. The oldest procedure for constructing a conventional tailings disposal corresponds to the upstream method. In the past it has been by far the most commonly used method of tailings dam construction because it needs lesser fill material. The upstream dam construction is associated with the direction in which raised dike moves in relation to the previous dike. The dikes or embankments are constructed with the sandy fraction of the tailings (cycloned tailings sand) and founded on the finer tailings stored on the pond (Fig. 16).

Due to the negative experiences of catastrophic flow failures of tailings dams constructed by the upper stream method, the present Chilean provision associated with tailings dam projects explicitly indicates that this construction method is prohibited. However, as the Las Palmas tailings dam, there is a substantial

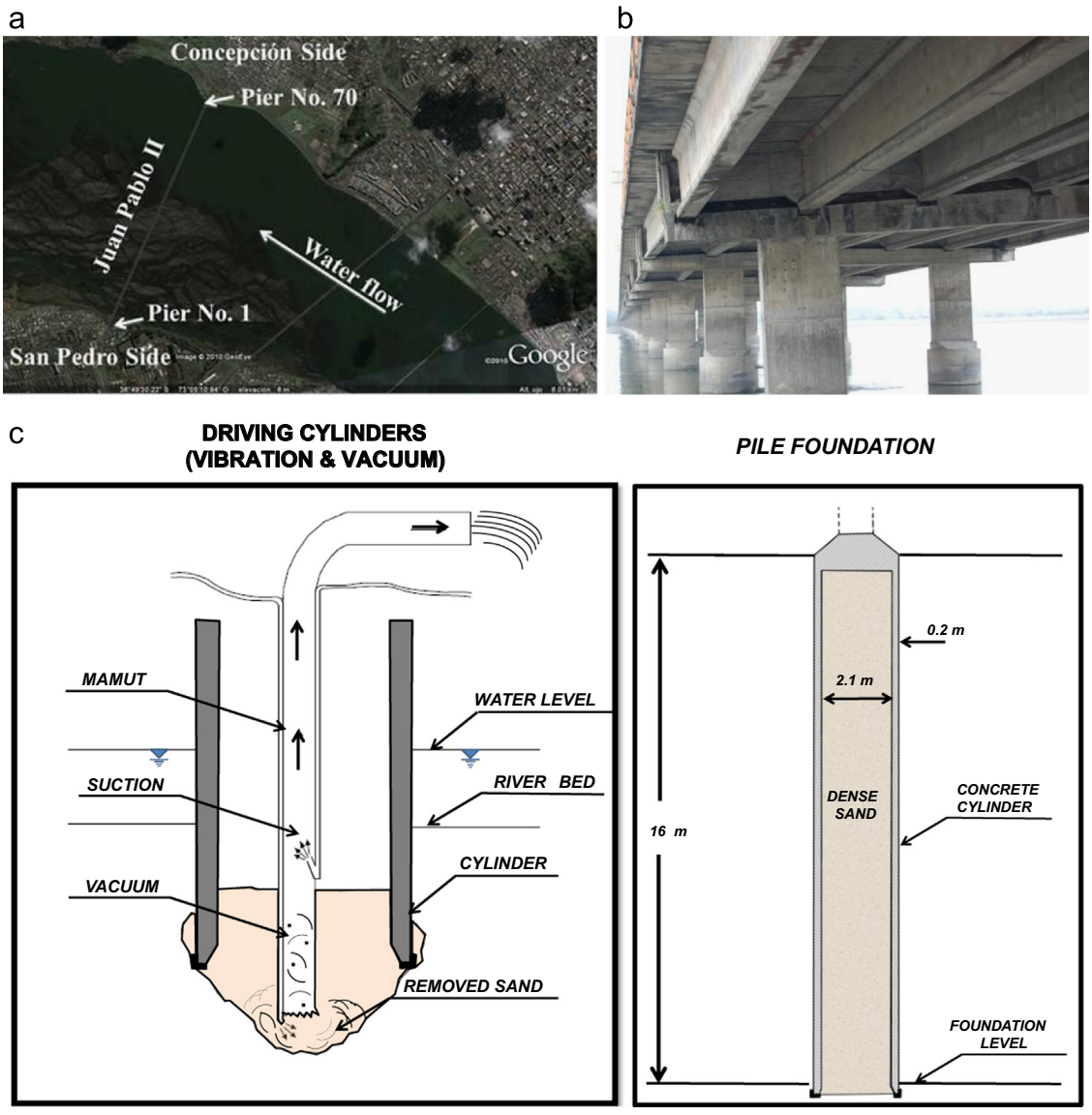

Fig. 19. (a) Location of Juan Pablo II Bridge, (b) Settlement of supporting structure and (c) Construction System and Pile Foundation.

Fig. 20. Settlements along Juan Pablo II Bridge with no evidence of horizontal displacements.

number of abandoned upstream raised dams constructed along the country before the provision, which represent a considerable risk to the population living within the runoff distance. Probably this is a common issue shared with other countries where old mining operations have left unsafe tailings disposals that are difficult to identify as well as to control.

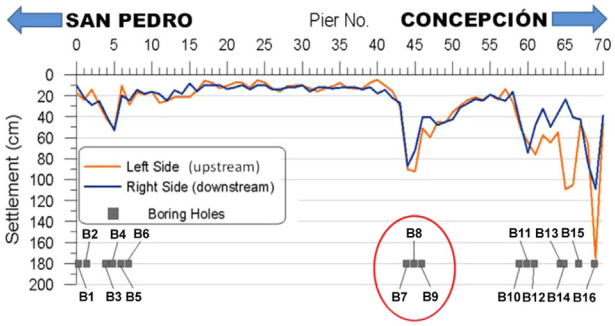

Fig. 21. Measured settlements along the Juan Pablo II Bridge.

6.3. *Lateral spreading of gentle slopes*

The fieldwork observations suggest that lateral spreading is the most systematic manifestation of liquefaction. In some locations, longitudinal cracks associated with the lateral spreading were continuously observed for a couple of kilometers along the banks of rivers. Typical examples of damages generated by lateral spreading on gentle natural slopes are shown in Fig. 17a and b, where superficial blocks of dry soil broke up internally, moving downward and "floating" on top of the liquefied layer. In general, the geometry of the ground under a lateral spreading condition can be characterized by a length, L, and a width, D. As it is sketched in Fig. 17c, the length, L, represents the distance of the spreading

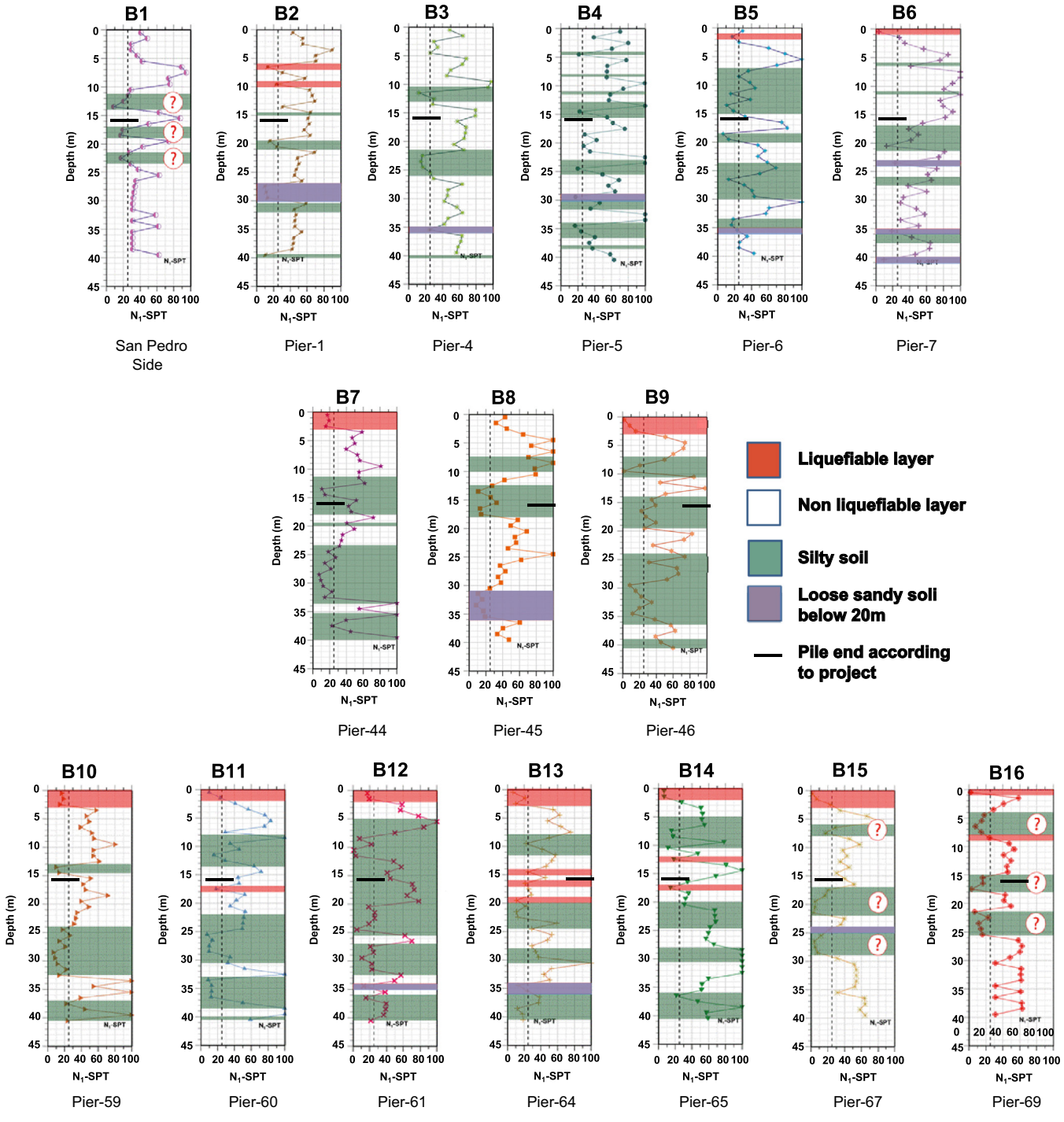

Fig. 22. Normalized N_1-SPT values at Juan Pablo II Bridge.

ground parallel to the shoreline, while the width, D, represents the inland extension of the spreading ground. Initially, the authors evaluated a possible correlation between these two geometrical parameters; however, the empirical evidence left by the 2010 Chilean Earthquake, clearly indicated that other variables (natural slope, thickness of superficial non-liquefied crust, extension of liquefiable soil, among others), have a strong influence in the resulting geometry. Therefore, any attempt to correlate L and D has to consider a site-specific analysis.

6.4. Failures of pile foundations due to lateral spreading

Pile foundations of several port facilities were damaged by the action of liquefaction-induced lateral spreading as shown in Fig. 18. This phenomenon has been observed and widely studied [21–23]. This type of damage is usually associated with a high economic cost, which is primarily caused by the halted operations of the port structures supported by piles. It is important to bear in mind that the costs of operation disruption of ports or electrical power plants are an order of magnitude greater than the cost of reparations.

6.5. Juan Pablo II bridge

Juan Pablo II Bridge crosses the BioBio River, connecting Concepción and San Pedro (Fig. 19a). Its construction began in 1968 and in 1974 started to operate. The bridge has a total length of 2310 m, a width of 21.9 m with a total of six lanes. It is structured by means of 70 spans, each composed of seven reinforced concrete girders and a concrete deck. Each span is supported by reinforced concrete columns, connected to driven cylinder piers of 2.5 m in diameters and 16 m in length (Fig. 19b).

After the 2010 Chile Earthquake clear evidence of liquefaction-induced lateral spreading in the Northern abutment (access to Concepción) was observed [24]. However, the piers located into the river bed did not present any evidence of lateral displacements, but important settlements due to the occurrence of liquefaction were observed (photos of Fig. 20). The magnitudes of the vertical displacements along the bridge are shown in Fig. 21. Larger settlements developed at the Concepción abutment bank. The largest settlement is about 1.8 m, followed by settlements of 1.1 m and 0.9 m.

An exploration consisting on a series of 16 boreholes with SPT-N measurements was carried out by the Chilean Ministry of Public Works. An energy ratio of 60% was assumed considering that the Chilean procedure follows the U.S. testing practice. The resulting values of $(N_1)_{60}$ are plotted in Fig. 22.

It has been estimated that values lower than 25 blows per foot are associated with liquefiable sandy soil layers, and colored in red (Fig. 22). Disturbed soil samples, recovered in the SPT spoon (sample tube), were tested in the laboratory to classify the materials. Grain size, specific gravity and Atterberg Limit tests were carried out. Consistently, the characteristics of the fine-grained materials did not permit the evaluation of their Plastic Limit. Accordingly, they were classified as non-plastic silts. The layers of non-plastic silty materials are marked in green. Considering that below 20 m, the occurrence of liquefaction could be doubtful, the sandy layers with low SPT blowcount located below 20 m have been identified as loose sandy soil below 20 m.

According to the available information of the original project, the piers had to be pushed down 16 m below the river bed. Therefore, the piers 45, 46, 67 and 69 would be resting on silty soft materials and piers 60, 64 and 65 would be in contact with liquefiable sandy soils. With the exception of pier 44, there is a good agreement between the observed settlements and the soil conditions established from the SPT-N data. Accordingly, these results show that non-plastic silts were also affected by the occurrence of liquefaction under the strong seismic load imposed by the 2010 Chile Earthquake.

It is interesting to realize that although important settlements occurred on several piers, no permanent transverse horizontal displacements were observed along the bridge. This fact necessarily implies that non-liquefiable layers were able to provide sufficient lateral stiffness and strength to ensure the transverse lateral stability of the bridge. From a point of view of the structural design, this is a crucial issue because it reduces considerably the required sub-structure to guarantee the lateral stability.

According to the boreholes, the stratigraphic profile is constituted by a multilayer sequence of soft soil and loose and dense sands. This strong stratification is common in the soil deposits existing in the Intermediate Depression. Probably, the high seismic activity of the region plays a role in this stratification. The seismic history of any site should be necessarily associated with liquefaction of those initially loose sandy soil deposits. These episodes have the singularity of modifying their structure and to likely transform them in highly heterogeneous soil deposits, in terms of density. Therefore, a layered structure that would consist of loose and dense soil layers is expected, which means a stratified structure of liquefiable and non-liquefiable layers.

In fact, the existence in Chile of natural soil deposits composed of several meters of just loose sandy soil is extremely rare. On the contrary, highly stratified sandy soil deposits consisting of loose and dense layers are usually encountered. Therefore, only two types of sandy soil deposits should be possible: in dense state, without any problem of liquefaction, and strongly stratified state, with liquefiable and non-liquefiable soil layers.

7. Evidence of recurrent liquefaction

Comparing the history of liquefaction of previous seismic events with the present database of 2010 Earthquake, several sites with recurrence of liquefaction were identified. This empirical

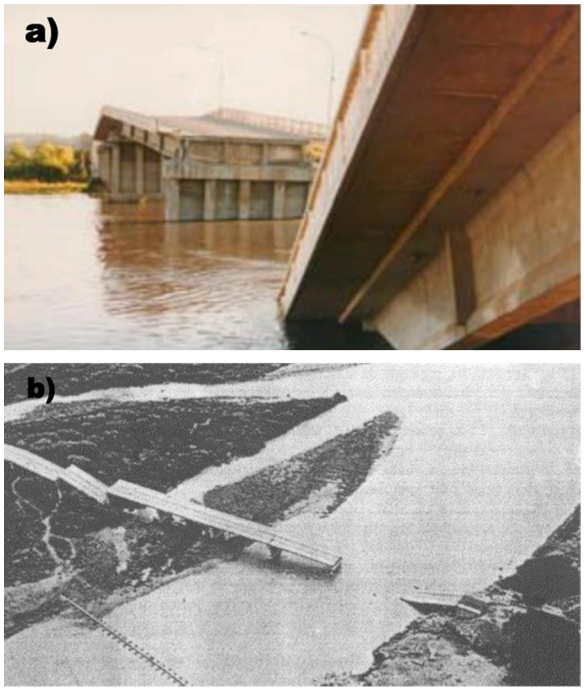

Fig. 23. Collapse of Lo Gallardo Bridge after the 1985 Earthquake (a) Pier settlement (M. Astroza) and (b) General view of the failures [26].

evidence confirms that a liquefiable site may experience liquefaction several times. This condition of sites with recurrent liquefaction has been also observed after the Great East Japan Earthquake of March 11, 2011 [25].

One clear example is the site, Muelle Schuster, located in Valdivia and shown previously in Fig. 12. Another case occurred in the mouth of the Maipo River, approximately 90 km south-west of Santiago. During the 1985 Earthquake, the first three spans adjacent to the right abutment (North) of Lo Gallardo Bridge collapsed due to the occurrence of liquefaction (Fig. 23). The bridge constructed in 1958 consists of 28 simple-supported spans, each 30 m long [26]. The damaged piers consisted of five square columns of 1 m thickness supported by 17 precast concrete piles, each 14 m long (Fig. 24a). The bridge was repaired after the 1985 Earthquake by means of additional piles to a depth of 25 m. As can be observed in Fig. 24b, these additional piles were installed laterally, connecting them to the original foundation system by enlarging the pile caps. Due to the 2010 Chile Earthquake it underwent some lateral deformations, as can be observed in Fig. 25, which is a symptom of the re-occurrence of liquefaction.

The Hospital overpass, located approximately 45 km to the south of Santiago, presented some degree of damages after the 1985 Earthquake, suggesting that a limited liquefaction could have happened. Due to the 2010 Earthquake, severe damages resulting

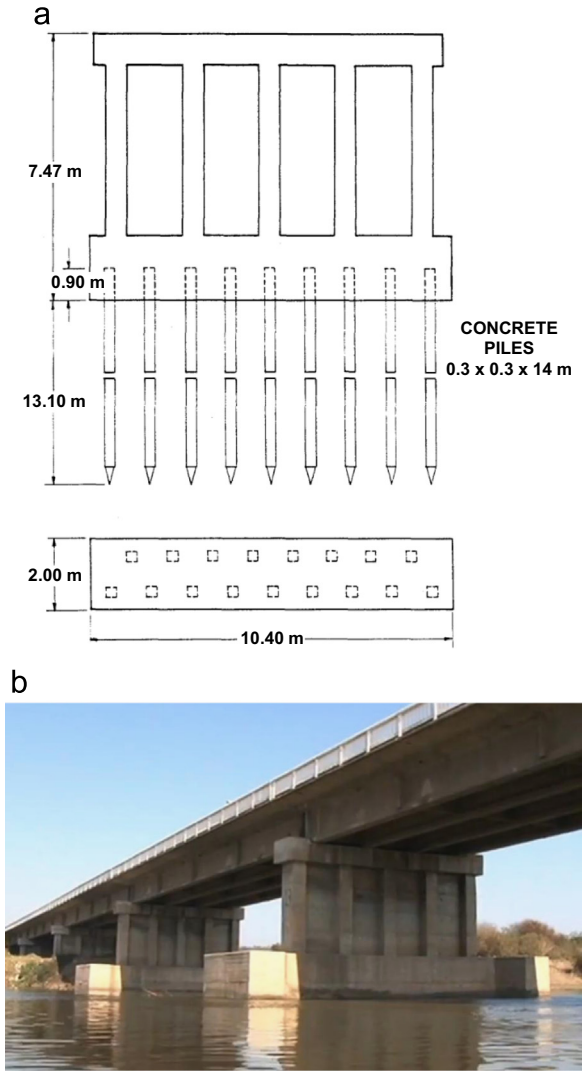

Fig. 24. (a) Plan and elevation of original piers (modified from [26]) and (b) Repaired piers after 1985 Earthquake (Videos MOP).

Fig. 25. Misalignment of Lo Gallardo Bridge (TV San Antonio).

Fig. 26. Collapse of Hospital overpass.

from liquefaction caused the collapse of this overpass (lane with north direction). A maximum permanent horizontal displacement of 87 cm was measured at the north abutment, which triggered the fall of the bridge deck (Fig. 26). The stratigraphy of the ground, shown in Fig. 27, indicates the existence of saturated loose layers of sandy soils characterized by SPT blowcount of less than 20. These sandy layers are enclosed by fines soils, which generate an optimum condition for an undrained behavior. To reproduce the observed permanent horizontal displacement, the sandy layers have to be considered completely liquefied with their residual undrained strength [27]. In this case, the previous earthquake of 1985 only induced a limited liquefaction and its recurrence was activated by the 2010 Earthquake of Magnitude 8.8.

8. Concluding remarks

On February 27, 2010, a mega thrust-faulting type earthquake of Magnitude 8.8 hit the Central-South region of Chile. The rupture

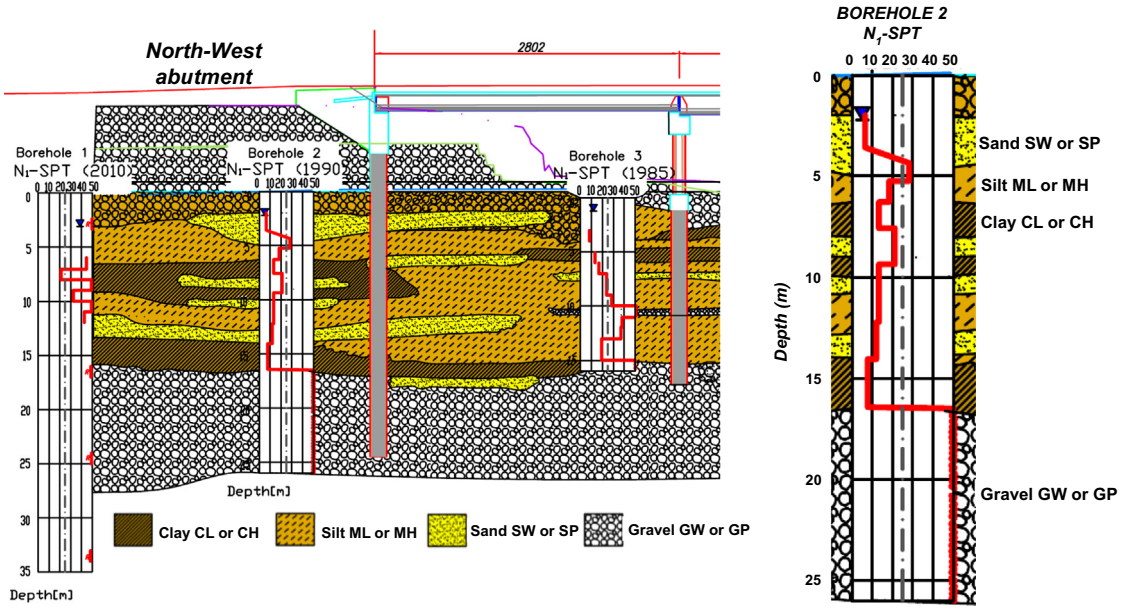

Fig. 27. Stratigraphy at North-West abutment (modified from [27]).

zone covered a rectangular area of approximately 550 km by 170 km, with an average depth of 35 km, overlapping the rupture zone of the 1960 Valdivia earthquake towards south and, at some extent, limited by the 1985 Valparaíso earthquake rupture towards north.

Maximum crustal co-seismic deformations were recorded at the tip of Arauco Peninsula, with an uplift of 1.8 m and a horizontal movement towards the trench of 5.1 m. Considering that the occurrence of liquefaction, among other factors, is controlled by the shaking duration, this parameter was computed for each available acceleration record. The results indicate that the records with the longest durations are located in the same area of maximum crustal co-seismic deformations. This finding suggests that for mega earthquakes, where co-seismic deformations are significant, the shaking duration varies according to the distance to the maximum crustal deformations.

Liquefaction sites were observed along the country, covering an extension close to 1000 km, which approximately represents twice the length of the rupture zone. The farthest site with evidence of liquefaction was recognized at Llanquihue Lake, located at 550 km and 350 km from the epicenter and fault, respectively.

The 2010 Chile Earthquake confirmed that tailings dams built using the upstream construction method are unsafe under seismic events. Although the provisions prohibit this construction method, there are numerous abandoned tailings dam that were constructed by such method, which are seismically unstable. This situation is common to many countries, so significant efforts must be done by governments in order to identify and prevent tailings failures.

In high seismic environments, any sandy soil deposit, initially loose, should undergo liquefaction during its geological time. The repetitive seismic episodes should modify the initial structure, generating highly heterogeneous soil deposits in terms of density. Therefore, a stratified structure consisting of a sequence of loose (liquefiable) and dense (non-liquefiable) soil layers could be expected.

The empirical evidence left by the 2010 Chile Earthquake confirms that liquefiable sites reiteratively experience liquefaction.

Acknowledgments

The authors want to acknowledge the very useful comments done by Dr. Javier Ubilla. Additionally, all the support provided by CMGI Ltda. and Department of Civil Engineering of University of Chile is gratefully appreciated, especially during the reconnaissance carried out after the 2010 Chile Earthquake.

References

[1] Ruiz S, Madariaga R, Astroza M, Saragoni R, Lancieri M, Vigny C, et al. Short-period rupture process of the 2010 Mw 8.8 maule earthquake in Chile. Earthq Spectra 2012;28:S1–18.
[2] Vigny C, Socquet A, Peyrat S, Ruegg JC, Métois M, Madariaga R, et al. The 2010 Mw 8.8 Maule megathrust earthquake of central Chile, monitored by GPS. Science 2011;332:1417–21.
[3] Renadic: Red Nacional de Acelerógrafos Departamento de Ingeniería Civil. Universidad de Chile. ⟨http://www.terremotosuchile.cl/⟩.
[4] C.S.N.: Centro Sismológico Nacional. Universidad de Chile. ⟨http://www.sismologia.cl/⟩.
[5] Bolt, B.A. Duration of strong motion. In: Proceedings of the 4th World Conference on Earthquake Engineering, Santiago, Chile; 1969. p. 1304–1315.
[6] Trifunac MD, Brady AG. A study on the duration of strong earthquake ground motion. Bull Seismol Soc Am 1975;65(3):581–626.
[7] Boore DM. Stochastic simulation of high-frequency ground motions based on seismological models of the radiated spectra. Bull Seismol Soc Am 1983;73 (6):1865–94.
[8] Kempton J, Stewart J. Prediction equations for significant duration of earthquake ground motions considering site and near-source effects. Earthquake Spectra 2006;22(4):985–1013.
[9] Arias A. A measure of earthquake intensity. In: Hansen RJ, editor. Seismic Design for Nuclear Power Plants. Cambridge, Massachusetts: MIT Press; 1970. p. 438–83.
[10] Moreno M, Melnick D, Rosenau M, Baez J, Klotz J, Oncken O, et al. Toward understanding tectonic control on the Mw 8.8 2010 Maule Chile earthquake. Earth Planet Sci Lett 2012;321-322:152–65.
[11] Dobry R, Idriss I, Ng E. Duration characteristics of horizontal components of strong motion earthquake records. Bull Seismol Soc Am 1978;68(5):1487–520.
[12] Midorikawa S, Miura H, Atsumi T. Characteristics of strong ground motion from the 2011 gigantic Tohoku, Japan earthquake. In: The International Symposium for CISMID 25th Anniversary; 2012. Paper No. M-4.
[13] Corvalan J, Herve F. Geological origin of Chile. Large Dams in Chile. Santiago, Chile: CIGB - ICOLD; 1996. p. 33–46.
[14] Ambraseys NN. Engineering seismology. Earthq Eng Struct Dyn 1988;17:1–105.
[15] Rathje E, Bachhuber J, Cox B, French J, Green R, Olson S, et al. Geotechnical engineering reconnaissance of the 2010 Haiti Earthquake. GEER Association Report No. GEER-021; 2010. Chapter 7.

[16] Ishihara K. Liquefaction in Tokyo Bay and Kanto regions in the 2011 Great East Japan Earthquake. In: Proceedings of the international symposium on engineering lessons learned from the 2011 Great East Japan Earthquake, Japan; 2012. p. 63–81.
[17] Verdugo R, González J, González V, Torres A. Características y efectos del fenómeno de licuefacción. Mw=8.8 Terremoto en Chile, 27 de Febrero 2010. . Department of Civil Engineering, University of Chile; 2012. p. 63–105 in Spanish.
[18] Verdugo R, Sitar N, Frost JD, Bray JD, Candia G, Eldridge T, et al. Seismic performance of earth structures during the February 2010 Maule, Chile, earthquake: dams, levees, tailings dams, and retaining walls. Earthq Spectra 2012;28(S1):S75–96.
[19] Bray JD, Frost JD, Rathje EM. Turning disaster into knowledge. ASCE G-I GeoStrata 2011:18–26.
[20] Bray J.D., Frost J.D., Eds. Geo-Engineering Reconnaissance of the 2010 Maule, Chile Earthquake. A report of the NSF-sponsored GEER Association Team; 2010. p. 327–330.
[21] Berrill JB, Christensen SA, Keenan RJ, Okada W, Pettinga JR. Lateral-spreading loads on a piled bridge foundation. Seismic behavior of ground and geotechnical structures. In: Proceedings of the special technical session on earthquake geotechnical engineering, 14th ICSMFE, Rotterdam; 1997. p. 173–83.
[22] Tokimatsu K. Performance of pile foundations in laterally spreading soils. In: Proceedings of second international conference on earthquake geotechnical engineering. Portugal; 1999 3. p. 957–64.
[23] Abdoun T, Dobry R, O'Rourke TD, Goh SH. Pile response to lateral spreads: centrifuge modeling. J Geotech Geoenviron Eng 2003;129(10):869–78.
[24] Ledezma C, Hutchinson T, Ashford S, Moss R, Arduino P, Bray J, et al. Effects of ground failure on bridges, roads, and railroads. Earthq Spectra 2012;28(S1): S119–S143.
[25] Wakamatsu K. Recurrent liquefaction induced by the 2011 Great East Japan Earthquake compared with the 1987 Earthquake. In: Proceedings of the international symposium on engineering lessons learned from the 2011 Great East Japan Earthquake, Japan; 2012. p. 675–86.
[26] Earthquake Engineering Research Institute (EERI). The Chile Earthquake of March 3, 1985. Earthquake Spectra; 1986 2 (2). p. 273–291, 411–427.
[27] González V, Verdugo R. Licuefacción en el area de Paine inducida por el Terremoto 27F. VII Congreso Chileno de Geotecnia. Concepción 2012 in Spanish.